



HAL
open science

DFT studies of 2-mercaptobenzothiazole and 2-mercaptobenzimidazole as corrosion inhibitors for copper

Eléa Vernack, Dominique Costa, Philippe Tingaut, Philippe Marcus

► **To cite this version:**

Eléa Vernack, Dominique Costa, Philippe Tingaut, Philippe Marcus. DFT studies of 2-mercaptobenzothiazole and 2-mercaptobenzimidazole as corrosion inhibitors for copper. *Corrosion Science*, 2020, 174, pp.108840. 10.1016/j.corsci.2020.108840 . hal-03453314

HAL Id: hal-03453314

<https://hal.science/hal-03453314>

Submitted on 16 Nov 2022

HAL is a multi-disciplinary open access archive for the deposit and dissemination of scientific research documents, whether they are published or not. The documents may come from teaching and research institutions in France or abroad, or from public or private research centers.

L'archive ouverte pluridisciplinaire **HAL**, est destinée au dépôt et à la diffusion de documents scientifiques de niveau recherche, publiés ou non, émanant des établissements d'enseignement et de recherche français ou étrangers, des laboratoires publics ou privés.

DFT studies of 2-mercaptobenzothiazole and 2-mercaptobenzimidazole as corrosion inhibitors for copper

Author and co-author contact information

Eléa Vernack^{a,b,*}, Dominique Costa^{a,*}, Philippe Tingaut^b and Philippe Marcus^a

^aPSL Research University, Chimie ParisTech-CNRS, Institut de Recherche de Chimie Paris (IRCP),
Research Group Physical Chemistry of Surfaces, 75005 Paris, France

^bSOCOMORE, 56000 Vannes, France

*corresponding authors

Abstract

This work describes 2-mercaptobenzothiazole (MBT) and 2-mercaptobenzimidazole (MBI) adsorption on Cu(111) by a systematic DFT study. Whatever the surface coverage of the adsorbed molecule, the adsorption is favored when the exocyclic sulfur atom is unprotonated (i.e. thione and thiolate forms). At low molecular density, the molecules adsorb forming a Cu-S(exo) and a Cu-N bond, and the adsorption energies of both molecules are similar, around 1.2 eV. To investigate a coverage corresponding to the density of self-assembled films, two strategies were applied: on the one hand, the best epitaxial relationship between the molecular layer and the Cu(111) surface was searched. A reasonable accommodation was found for a molecular density of 3.9 **molecule**/nm² in the honeycomb (3x3) Cu(111) superstructure, in which the molecules are adsorbed with the C_{2v} axis tilted, forming two Cu-S bonds for MBT and one Cu-S and one Cu-N bond for MBI. On the other hand, the best structure for atomic S on Cu(111), the ($\sqrt{7} \times \sqrt{7}$) R19° superstructure, with a molecular coverage of 5 **molecule**/nm², was considered. We find that the honeycomb MBT and MBI layer is the most stable arrangement, showing that in this case, the molecular organization prevails over the head-group/surface interaction. The MBI molecule adsorbs more strongly than the MBT molecule, due to better lateral interactions in the organic layer.

Keywords

- A. Copper
- B. Modelling studies
- C. Interfaces

1. Introduction

Corrosion is a worldwide phenomenon that affects many industrial sectors (transport, infrastructure, health...) and has huge economic impacts. Its prevention is thus a crucial issue. A solution to avoid this phenomenon is the use of corrosion inhibitors. Several molecules are cited in the literature as good corrosion inhibitors, but they are often expensive, unstable, or dangerous for humans and/or the environment. Hexavalent chromium is an example of very efficient corrosion inhibitor, currently used in industry, but it is highly toxic [1] [2]. Researches of new inhibitors and especially of « green » inhibitors are booming [3] [4] and quantum calculations could be a promising approach to lead these researches [5] [6] [7]. Calculations are now often used to describe molecular properties and molecule-surface interactions to understand corrosion inhibition properties. Density functional theory (DFT) calculations are particularly used in this field because they enable to model surfaces covered by self-assembled monolayers of molecules. Indeed, previous works demonstrated that the study of the properties of the molecule alone (without interaction with the surface) is not sufficient to explain or predict different inhibitor properties. SAM (self-assembled monolayer) and molecule-metal interactions have to be considered to define some realistic descriptors and to understand corrosion inhibition mechanisms [8] [9] [10].

We join theoretical and experimental studies of the corrosion inhibition properties of 2-mercaptobenzothiazole (MBT) and 2-mercaptobenzimidazole (MBI) on copper. We chose a copper surface as a model which permit us to predict corrosion inhibitor behaviors of molecules on this surface but also on some sensitive alloys which contain this metal (for example: 2024 aluminum alloy sensitive to corrosion due to the presence of copper). This part is dedicated to the theoretical study. Both molecules are well known in the literature to have a good efficiency on copper surfaces, but their adsorption mechanisms are still discussed. For example, Marconato *et al* [11] and Shahrabi *et al* [12] studied MBT properties on copper in acidic media. Both demonstrated that MBT acts as cathodic and anodic type inhibitor, but they described two different adsorption mechanisms. Marconato *et al* explain in their works that MBT protects copper surfaces by forming Cu^+MBT complexes precipitated on the surfaces while Shahrabi *et al* explain that MBT adsorption is due to non-covalent bonds (electrostatic bonds). They made the same conclusion for MBI. Kazansky *et al* [13] determined that in neutral phosphate media, MBT adsorbs on copper through its nitrogen and exocyclic sulfur atoms forming a protective monolayer on the surface. They also explained that the thickness of this layer increases with time. Thanks to XPS analysis, Finsgar *et al* [14] [15] determined a similar mechanism for MBT and MBI in chloride media. They also demonstrated that MBT acts on both anodic and cathodic reactions. Additional works demonstrated that MBI has a similar adsorption mechanism. Xue *et al* [16] determined, thanks to X-AES and IR analysis, that nitrogen and sulfur atoms are involved in the adsorption mechanism of MBI and such a layer is stable and protective in acidic and alkaline media. Subramanian *et al* [17] showed that in alkaline solutions, the ionization of the exocyclic sulfur promotes the adsorption of the MBT molecules that form a polymeric, thick and protective layer. Chadwick *et al*

[18] also studied the layers formed by MBT and MBI on copper in a chloride solution and demonstrated that both films degraded with time due to the presence of dioxygen which lead to the formation of Cu (II) cations and the dimerization of the molecules. Several years later, Li *et al* confirmed these results with MBT [19].

Some DFT studies were also dedicated to MBT and MBI molecules adsorption on Cu. We can cite the works conducted by Sun *et al* [20] in 2012 who modelled a MBI molecule adsorbed on a Cu(111) surface. They used DFT to calculate adsorption energies depending on the orientation of the molecule, with neutral and dehydrogenated forms of MBI. They showed that the neutral molecules on the metal surface chemisorbed in a perpendicular configuration and physisorbed in parallel configuration whereas the dehydrogenated molecules chemisorb on the surface. The authors used electronic analysis to determine that both nitrogen and sulfur atoms are involved in the chemisorption of MBI. They connected the adsorption energy with corrosion inhibition properties and compared MBI with otherazole derivatives. Obot *et al* [21] also studied by DFT and molecular dynamics (MD) simulations the adsorption of MBI on Cu(111) at low molecular density. Their conclusion was different than that of Sun. Indeed, they found that the thione form of MBI is more stable and more reactive than the thiol form. MD simulations showed that the molecule-surface interaction is only in a parallel configuration. This orientation is explained by the fact that the population distribution of the HOMO and LUMO orbitals is relatively homogeneous over the molecule and the reactive sites are shared between the sulfur and nitrogen atoms and the π electrons of the molecule. Kovačević *et al* [22] also used DFT calculations to explain the corrosion inhibition properties of five imidazole molecules including MBI. They confirmed that the thione form is more stable than the thiol form in vacuum but also in aqueous phases, by about 0.1 to 0.3 eV. They demonstrated that the S-H bond can be more easily broken than the N-H bond and so thiols are prone to dissociation upon adsorption. They calculated that the S-H bond of thiol molecules dissociates in about 1 nano-second on the surface. So, they concluded that the thiol form of MBI can be dissociated to form the thiolate form which adsorbs more strongly on the surface. They stated that thione forms are less prone to dissociation: the corresponding dissociation activation energy is about 0.9 eV whereas is equal to about 0.2 eV for thiol molecules. Furthermore, they confirmed results from previous works showing that the nitrogen and sulfur atoms are involved in the adsorption of MBI with a tilted orientation. They also showed that the adsorption energy is not a sufficient parameter to explain the experimental results. To complete these results, they also studied the formation of MBI/Cu²⁺ complex and their solubility in aqueous solutions. They concluded that in contrast to other molecules, MBI molecules do not react with Cu²⁺ ions to form soluble complexes that would promote corrosion. It is important to note that in all these works, adsorption at low molecular density was considered to well understand the molecule surface interaction.

Following a standard QSAR (Quantitative Structure Activity Relationship) approach, the electronics properties of the molecules have been investigated and correlated with their inhibition effect. Several authors found a good correlation between electronic properties of isolated molecules and corrosion

inhibition properties. For example, in 2012 Niamien *et al* compared inhibition efficiency (IE) on copper of three imidazole derivatives (experimental results) with their electronic properties determined by quantum calculations [23]. They established linear relationships between IE and ΔE (ΔE being the adsorption energy), IE and ΔN (ΔN being the fraction of electrons transferred from the molecule to the metal). In 2015, Awad *et al* used a similar method to compare four triazole derivatives adsorbed on aluminium [24]. They also demonstrated a good correlation between experimental results and electronic properties. The analysis of electronic properties of isolated molecules could be a first indicator to define inhibition efficiency but several studies demonstrated that it is not sufficient to describe precisely the reactivity between molecules and a surface which is a more complex. One example to illustrate this point is the work led by Kokalj *et al* [8] [9] [10]. They demonstrated that even if benzotriazole and 1-hydroxybenzotriazole have similar electronic properties they do not have the same IE on copper (benzotriazole being more efficient). To explain such a difference, they showed that benzotriazole, due to its flat structure, can form a dense and stable monolayer on the surface by strong intermolecular bonds. In contrast, 1-hydroxybenzotriazole, with its OH functional group out of plane, forms a less dense layer, providing less protection against corrosion.

While many experimental studies conclude to the formation of layers of MBI and MBT on copper, to the best of our knowledge, no theoretical studies were performed to examine the adsorption of full layers of MBT and MBI on copper surfaces considering all the following parameters: chemical structures of the molecules, molecular density and anchoring mode of the molecules on the surface. We aim here to clarify these points. The strategy employed was to study: i) the properties of the isolated molecules, ii) the adsorption of isolated molecules on the Cu surface and iii) the formation of full layers adsorbed on Cu. The three conformers (i.e.: thiol, thione and thiolate forms) of the molecules were considered.

2. Calculation parameters

All calculations were performed using the periodic density functional theory method (DFT). This method is based on the GGA approximation [25] employing the PBE exchange-correlation functional [26] as implemented in the plane-wave program Vienna ab initio simulation package (VASP) [27] [28] [29]. The projector-augmented wave (PAW-PBE) potentials [30] were used for the core electron representation.

To perform calculations and guarantee their quality and precision, we used an energy cutoff E_{cut} equal to 520 eV. D2 Grimme approach was used to consider dispersion forces [31]. It is known now that DFT-D2 method overestimates the molecule/metal dispersion interactions. A more elaborate method [32], the DFT-D3 method, also exists but it was not used this work. It contains an additional corrective factor: indeed, the method tries to empirically estimate three-body interactions whereas DFT-D2 method consists of two-body interactions only. So, to confirm our results obtained with DFT-D2 method, we also used D3 Grimme approach for the most stable configurations and especially those allowing us to

determine the most stable organized films on the surface. The adsorption energies determined by using both methods are similar to within 0.05 eV, not changing our conclusions.

The isolated molecules were optimized in a 15x15x15 Å³ cell at the Gamma Point. The molecules were oriented with the backbone parallel to the Z axis, to calculate the Z component of the dipolar moment of the isolated molecule and compare it to that of the full layer. To compare the electronic properties of the isolated molecule in the gas phase (HOMO and LUMO) with that of the surface (Fermi level), we took the vacuum as the reference of energy.

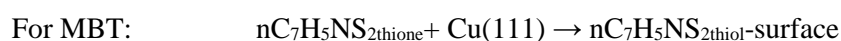
The optimization of bulk Cu at the PBE level gave a cell parameter of 3.639 Å, in good agreement with the experimental value of 3.615 Å [33]. The Cu(111) slab was 5 layers thick with the two top layers relaxed and the three bottom layers frozen in the bulk position. A vacuum height of 22 Å was introduced. Several molecular densities of the adsorbed molecules were investigated: from relatively low density to a full molecular monolayer. To this end, we used different types of Cu(111) cells : a (2x2) cell, with a = b = 5.16 Å, a $\begin{pmatrix} 2 & 2 \\ 1 & -1 \end{pmatrix}$ cell with a=6.82 Å, b=4.48 Å, a ($\sqrt{7} \times \sqrt{7}$) R19° cell, **with the a and b lattice a = 6.82 and b= 6.82 Å**, a (3x3) Cu(111) cell, with the a and b parameters both 7.73 Å, an orthorhombic $\begin{pmatrix} 2 & 3 \\ 2 & -3 \end{pmatrix}$ supercell of dimensions 8.91x7.72 Å², and a (4x4) cell of dimensions a = b = 10.32 Å. The KPOINTS grid was adapted to the cell size. All cell names, unit vectors lengths, number of Cu surface atoms, cell area, KPOINTS grids are reported in Table S.I.-1. An increased mesh (6x6x2) was used for electronic analyses.

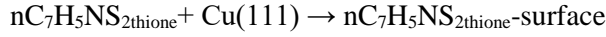
The adsorption of the MBT and MBI molecules was investigated in several configurations of adsorption: adsorption through one or two atoms forming bonds with Cu, which are noted 1-atom bond to Cu, or 2-atom bond to Cu. In the case where the molecules are 1-atom bonded to Cu, the atom is the exocyclic S atom. When the molecules are 2-atom bonded to Cu, the second atom can be the endocyclic S or N for MBT, and the unprotonated endocyclic N for MBI (thiolate). For MBT, we precise the nature of the 2-bond atoms to Cu, by e.g. (S,S) or (S,N).

It is known that the tilt angle of aliphatic molecules adsorbed at surface decreases with increasing coverage [34]. Thus, because the aim of this paper is to understand how MBT and MBI can form full layers at the Cu surface and protect the surface from corrosion, we focus here on adsorption modes where the tilt angle of the molecules with the surface normal are low.

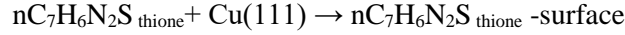
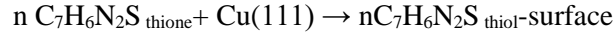
To calculate adsorption energies, we considered the following reactions, in which the reference for the molecule is in the thione form, which is more stable than the thiol form both in the gas and aqueous phase.

- For molecular adsorption, we considered:





For MBI:



and we calculate

$$\Delta E_{ads} = (E_{total} - E_{surface} - E(\text{molecule-thione}))/n \quad (1)$$

The adsorption energy is expressed in eV.

- For dissociative adsorption, i.e. adsorption of molecule in the thiolate form (with release of a hydrogen atom, the molecule being modeled in radical form R*), we write:



and we calculate

$$\Delta E_{ads} = (E_{total} - E_{surface} - E(\text{molecule-thione}) + n/2 E_{H_2})/n \quad (2)$$

where E_{total} is the energy of the whole system surface / molecule, $E_{surface}$ the energy of the surface alone, $E(\text{molecule-thione})$ the energy of the isolated molecule in the thione form, E_{H_2} the energy of the H_2 molecule.

For each calculation, the total energy contains a DFT and a VdW contribution. We can thus calculate the van der Waals contribution to the adsorption energy by applying the equations (1) or (2), but only with the Van der Waals contributions.

For the adsorption at full coverage, it is also interesting to calculate the cohesion energy in the adsorbed layer. To do this, we proceed as the following: we perform a single point energy calculation of the layer of molecules (MBT or MBI) in the geometry of the adsorbed layer, thus eliminating the underlying surface. The energy of cohesion is given by the formula:

$$E_{coh} = (E(\text{molecular-layer}) - n E(\text{molecule}))/n \quad (3)$$

where n is the number of molecules in the cell

In order to compare the respective stabilities of different high molecular density superstructures on the surface, this energy is also expressed by unit area, (in eV/nm²), which also corresponds to the difference of the surface energies before and after adsorption.

The dipole moments were evaluated using the Bader charges [35]. The dipole-dipole interactions were evaluated following the formalism developed in the work of Kovačević *et al* [36], who explains that the lateral dipole dipole interactions scale as μ^2/R^3 (μ is the dipole moment, R the interdipole distance). However, in the case of a layer of dipoles, the summation of all interactions results in an order of magnitude larger interaction energy per dipole (for not too anisotropic lattice), that is $E_{layer}^{dip} \approx 10 \mu^2/R_{nn}^3$ where R_{nn} is the nearest-neighbor distance between dipoles. This means that for dipoles of 4 D at the

R_{nn} distance of 40 bohrs the E_{dip} (layer) is on the order of 10 meV. We applied this formula to evaluate the repulsive contribution to the dipole-dipole interaction along the Z direction.

The difference in charge of the molecule before and after adsorption is calculated in making the difference between the Bader charge of the molecule (i.e. summing all contributions to the charge) before and after adsorption. Before adsorption, the charge is zero (the thiolate being considered in its radical form in the calculations), and after adsorption, the charge (generally negative) is the charge transferred by the metal surface.

3. Results and discussion

3.1. Study of the molecules

3.1.1. Isolated molecules in vacuum

The molecular structures of MBT and MBI depend on thermodynamic conditions. First, there is the tautomer equilibrium between the thiol form and the thione form of the thioamide functional group. Several studies have demonstrated that the thione structure is predominant when the molecules are in solid state and in many solvents including water [37] [38]. Recent studies even extend this observation to the gas phase [39]. In 1999, Sandhyarani *et al* also noted that the structure of MBT depends on the surface with which it is in contact. Indeed, while MBT adsorbs in the thione form on gold for example, it adsorbs in the thiol form on silver [40]. A second equilibrium is based to the acid-base properties of both molecules. Their deprotonation leads to the formation of conjugate bases (thiolate). The three structures were considered in our study.

We first modelled the isolated molecules in thiol and thione forms (Figure 1). Under these conditions (gas phase at 0 K), the thione form is more stable than the thiol form for both molecules (total energy of MBT thione form is 0.4 eV lower than MBT thiol form and MBI thione form is 0.6 eV lower than MBI thiol structure). We also determined some electronic properties, reported in Table 1, for each molecule (energy positions of highest occupied and lowest unoccupied molecular orbitals E_{HOMO} and E_{LUMO} , energy gap ΔE , electronegativity χ , electrophilicity ω , dipole moment μ , hardness η and softness σ).

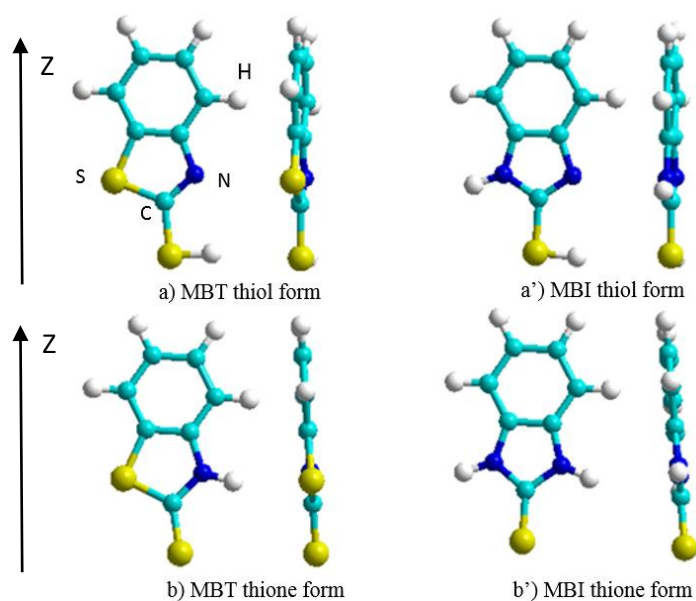


Figure 1: MBT and MBI molecules and their tautomer. The molecules are placed with the molecule backbone along the Z axis, which is perpendicular to the surfaces in the calculations of molecule adsorption on copper. Color code: light blue: C; dark blue: N; yellow: S; white: H atoms

Table 1: Energetic and electronic properties of MBT and MBI in thiol forms in the gas phase determined by DFT calculations. HOMO and LUMO energies are referred to the vacuum level.

	Relative energy of thiol with respect to thione (eV)	E_{HOMO} (eV)	E_{LUMO} (eV)	ΔE (eV)	χ (eV)	η	σ	ω
MBT thiol	0.4	-5.70	-2.09	3.6	3.9	1.8	0.6	4.2
MBI thiol	0.6	-5.31	-1.26	4.1	3.3	2.1	0.5	2.7

Several authors associate the electronic gap and the ionization potential (equal to $|E_{\text{HOMO}}|$) with the corrosion inhibition properties of molecules [23] [24]. A smaller gap (ΔE) indicates a greater reactivity of the molecule and therefore a better protection against corrosion. These studies also indicate that a more effective protection is obtained with molecules with the lowest ionization potential. Our results show that MBT has the lowest electronic gap, but the lowest ionization potential has been calculated for MBI. If we consider the value of E_{LUMO} , MBT is a better electron acceptor than MBI. MBI could react more strongly with copper surfaces because its E_{HOMO} (5.31 eV, calculated with the vacuum energy taken as the reference energy, zero) is closer to the Fermi level of the copper surface (given by the calculation of the electronic work-function to 4.96 eV with respect to the energy of vacuum). We also calculated the electronegativity χ , the electrophilicity index ω , the hardness η and the softness σ of both molecules. According to the value of the electronegativity, MBT would be more easily acceptor of

electrons although its hardness is lower than that of MBI. The electrophilicity index seems to indicate that electron transfer is easier with MBT than MBI. These values could be first indicators to determine molecule properties but for sure they are not sufficient, and they do not allow us to determine which molecule is the best corrosion inhibitor. The calculated dipole moments are reported in Table S.I.-2 for the three conformers of each molecule. The dipole moments of the two molecules are in the same range, ~ 3.3 D for the thione form and ~ 4.9 D for the thiolate form.

The solubility of MBT and MBI in water is low, 0.02 mol.L^{-1} (MBI), and $7 \times 10^{-2} \text{ mol.L}^{-1}$ (MBT). From these values we calculated solvation free energies ΔG values of $+0.10$ and $+0.19$ eV for MBI and MBT, respectively. The equations used are reported in S.I.-3. section. MBT and MBI have pKa of 6.9 and 10.4 respectively [41], meaning that in the domain of stability of metal Cu (non-oxidized) in water, (low pH), both molecules are present in the thione form in solution.

3.1.2. Standalone Self Assembled Monolayers on MBT and MBI

We then considered the properties of the organized monolayers of molecules without interaction with the copper surface. The modelling of close packed monolayers with molecules in different orientations (parallel to the Z direction and with the C_{2v} axis of the molecule tilted or not) shows that for both molecules, the most stable monolayer is formed when molecules are in a close packed hexagonal structure (Table 2, Figure 2). In this orientation, the molecules can form attractive but non-covalent interactions between their aromatic rings (Π -stacking) which stabilize the monolayer. The MBI layers have an increased cohesion energy as compared to the MBT SAM. We think that this is due to the presence of an additional H atom in MBI, and to the presence of two N atoms in the ring. The N atoms in the rings are negatively charged, -1.15 - -1.22 , whereas the S atom in the MBT ring is nearly not charged. This induces stronger electrostatic interactions between the H of NH and the neighbor N atoms (which are located at 2.9 \AA from the NH moiety). As a proof, we observe that the lateral interaction in MBI thione is still increased with respect to that of MBI thiol.

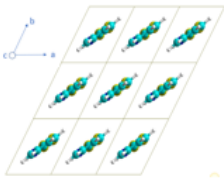
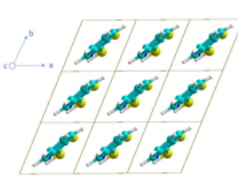
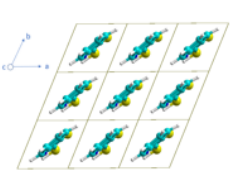
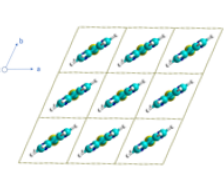
Molecule	MBT		MBI	
SAM form	SAM-thione	SAM-thiol	SAM-thione	SAM-thiol
Top view				
Density	4.6 molecule/nm ²	4.1 molecule/nm ²	4.5 molecule/nm ²	4.5 molecule/nm ²
Cohesion energy per molecule	-0.24 eV	-0.39 eV	-0.52 eV	-0.45 eV
Cohesion energy per surface area unit	-1.1 eV/nm ²	-1.6 eV/nm ²	-2.34 eV/nm ²	-2.02 eV/nm ²

Figure 2: Structures obtained for the most stable SAM (close packed) formed by MBT and MBI in thione and thiol forms. The densities and cohesion energies in the layer are reported. The cohesion energy is the energy difference between the molecule (thione or thiol) in the SAM and the same molecule in vacuum. The energy is reported per molecule, and, to compare the different SAM, per surface area unit. Color code: light blue: C; dark blue: N; yellow: S; white: H atoms

For the perpendicular thione SAM, the dipole moment is lower than that of the isolated molecule. The Z contribution of the dipole moment falls from ~ 3.3 for the free molecules to ~ 1.6 for the self-assembled molecules. The dipole-dipole repulsion thus represents only a weak part of the energetics, (0.3-0.5 eV) being counterbalanced by the attractive lateral-lateral interactions, and the lateral attractive dipole-dipole contributions. In the case of thiols SAM, the dipole moments are similar to that of the free molecules. The Z contributions to the dipole moment being weak, the dipole-dipole repulsion in the thiol layer is negligible.

Table 2: Molecular densities, cohesion energies and dipole moments of SAM formed by MBT and MBI

		Close packed thione	Thione, with the C _{2v} axis tilted	Close packed thiol
MBT	Density (molecule/nm²)	4.6	4.3	4.1
	Cohesion Energy per surface area (eV/nm ²)	-1.1	-0.64	-1.56
	Cohesion energy (eV)*	-0.24	-0.15	-0.39
	Dipolar moment (D, total/ Z projected)	2.1/1.7	-	5.3/0.2
	Dipole/dipole interaction (eV)	0.3	-	0
MBI	Density (molecule/nm²)	4.5	4.3	4.5
	Cohesion Energy per surface area (eV/nm ²)	-2.34	-1.13	-2.02
	Cohesion energy (eV)*	-0.52	-0.27	-0.45
	Dipolar moment (D, total/ Z projected)	1.8/1.5	-	5.0/0.2
	Dipole/Dipole Interaction (eV)	0.5	-	0

*The cohesion energy is the energy difference between the molecule (thione or thiol) in the SAM and the same molecule in vacuum

3.2. Adsorption of MBT and MBI on Cu(111) surface: low molecular density (1.5 **molecule/nm²**)

We considered several configurations as initial position: no atom, one atom and two atoms bonded to the surface. For each configuration, adsorbed molecules were modeled in their thiol, thione and thiolate forms. Figure 3 shows the different configurations considered in this paper. It should be noted that several adsorption sites have been systematically studied. Indeed, the atoms (sulfur or nitrogen) can adsorb on four different sites: on top, bridge, hollow hcp or hollow fcc. We found that the most stable site for atom adsorption is the hollow hcp site. The results obtained for the most stable configurations are reported in Table 3. Energetic results on other, less stable configurations are reported in S.I.-4 to 6 for thiol, thione and thiolate forms, respectively.

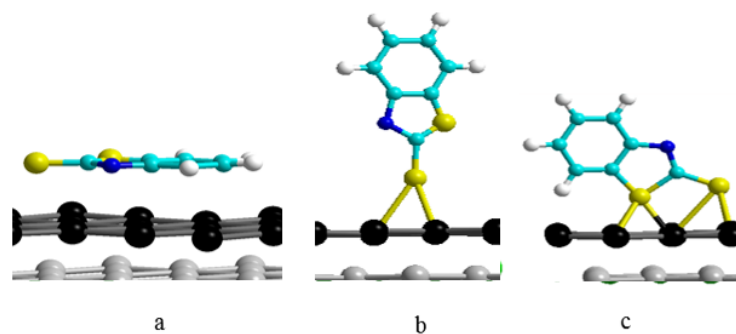


Figure 3: Representation of the different configurations modeled for the adsorption (shown here for MBT thiolate). The adopted nomenclature is a) no atom bonded to the surface, b) 1 atom bonded to the surface, c) 2 atoms bonded to the surface. In the last case, the molecule stands perpendicular to the surface, with the C_{2v} axis of the molecule tilted with respect to the surface normal. Color code: light blue: C; dark blue: N; yellow: S; white: H, black and dark grey: Cu atoms

Table 3: Most stable adsorption modes and adsorption energies of MBT and MBI on Cu(111) at low molecular density (1.5 molecule/nm²) in the orthorhombic $\begin{pmatrix} 2 & 3 \\ 2 & -3 \end{pmatrix}$ cell.

	Conformer	Thiol	Thione	Thiolate	
MBT	Adsorption mode	No atom bond	2-atom bond (S,S)	2-atom bond (S,S)	2-atom bond (S,N)
	Adsorption energy (eV)	-0.65 Equation (1)	-0.96 Equation (1)	-1.12 Equation (2)	-1.21 Equation (2)
	vdW contribution to the adsorption energy (eV)	-0.39	-0.54	-0.90	-0.73
	Molecule/surface distance (Å)	2.6	2.3	2.3	2.1 / 2.3
	Adsorption site	-	hollow	hollow	
	Figure	4.a	4.b	4.c	4.d
MBI	Adsorption mode	No atom bond	1-atom bond 2-atom bond	2-atom bond	
	Adsorption energy (eV)	-0.66 Equation (1)	-0.83 (S) -0.86 (S,N) Equation (1)	-1.25 Equation (2)	
	vdW contribution to the adsorption energy (eV)	-0.44	-0.2 (S) -0.37 (S,N)	-0.67	
	Molecule/surface distance (Å)	2.5	2.3 (S) 2.1-2.3 (S,N)	2.1-2.3	
	Adsorption site	-	hollow	hollow	

Figure	4.e	4.f and 4.g	4.h
--------	-----	-------------	-----

Figure 4 summarizes the energetics results for the most stable configurations obtained for each conformer. To allow the formation of bonds between the –N or –S moieties and the surface, a 1-atom bond (i.e; molecule parallel to the normal of the surface) or a 2-atom bond (i.e: with the C_{2v} axis tilted) adsorption mode is adopted. The results reported in table 3 (and in S.I.-4 and 5) show that all configurations are energetically stable ($\Delta E_{\text{ads}} < 0$ eV).

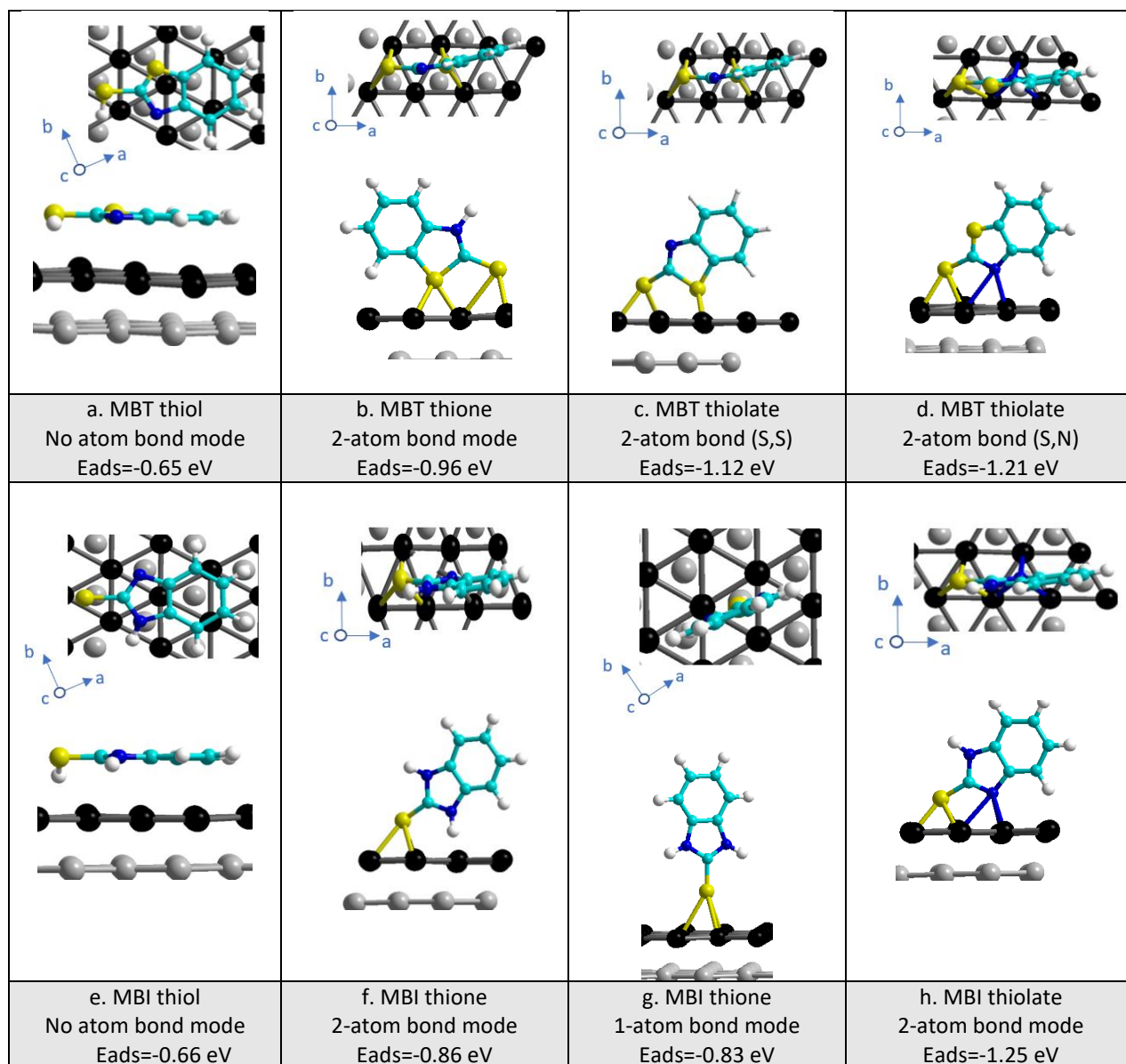


Figure 4: Most stable adsorption modes calculated for MBT and MBI on Cu(111), at 1.5 molecule/nm² molecular density, in the orthorhombic $\begin{pmatrix} 2 & 3 \\ 2 & -3 \end{pmatrix}$ cell. a-d) MBT, e-h) MBI. The adsorption energies are reported in Table 3. Color code: light blue: C; dark blue: N; yellow: S; white: H, black and dark grey: Cu atoms

We note that the adsorption is always stronger when the exocyclic sulfur is deprotonated (thione and thiolate) and able to form strong bonds with the surface (in other words, dehydrogenation of the

molecule to form a S_{exo} -Cu bond is an exothermic process). When the exocyclic sulfur atom cannot form strong bonds with the surface (i.e.: thiol conformers), the most stable configuration is when the molecule is parallel to the surface forming an angle of 90° with the normal of the surface, (no atom-Cu bond mode), whereas the thione and thiolate adsorb with a 1-atom and/or a 2-atom bond adsorption mode (the C_{2v} axis tilted and/or parallel to the normal of the surface). It appears clearly that for both molecules, the most stable configuration is obtained for the thiolate conformer in a 2-atom-Cu bonds mode (C_{2v} axis tilted configuration), the exocyclic S and a N atom being in a hollow site and forming Cu-S and Cu-N bonds. In the case of MBI, the N involved in a N-Cu bond is the unprotonated nitrogen atom. The interatomic distances between the atoms of the molecules and the copper surface are approximately equal to 2.3 Å for the S-Cu bonds and 2.1 Å for the N-Cu bonds. The present results are in good agreement with the results obtained by Sun *et al* [20] and Kovačević *et al* [22] who also demonstrated by DFT calculations that the most stable adsorption of MBI is in the thiolate form and with the C_{2v} axis tilted on the surface forming bonds through its sulfur and nitrogen atoms.

The adsorption energies of MBT and MBI are identical, being around -1.23 ± 0.02 eV, meaning that at room temperature, the adsorption of the molecules are isoenergetic.

With the 1-atom bond adsorption mode, the adsorption energy values in the thiolate form are -0.82 and -0.87 eV for MBT and MBI respectively (results described in Table S.I.-6). The similar adsorption energies can be explained by the fact that in these cases the adsorption is dominated by the formation of a sulfur (exocyclic)-copper bond. In comparison, we can cite the works of Geng *et al* [42] who studied the adsorption of benzene thiolate on a Cu(111) surface. They found that the benzene thiolate molecule adsorbs through its sulfur atom preferentially on a hollow fcc site with an adsorption energy of -2.26 eV/molecule and with a Cu-S distance equal to 2.3 Å. The authors considered the thiolate molecule as the reference for the adsorption energy. In our case, we calculate a binding energy between thiolate and Cu(111) of -2.56 (respectively -2.60) eV for MBT (MBI), thus in the same range of energy as calculated by Geng *et al*.

In the thione conformer, MBT adsorbs forming two S-Cu bonds. For MBI, the energies associated with the 2-atom bond adsorption mode (through S and N atoms) and 1-atom bond adsorption mode are practically equal. As a reminder, in the thione form, the two nitrogen atoms of MBI are bonded to a hydrogen atom. Thus, in the 2-atom bond adsorption mode (when the C_{2v} axis is tilted), the interaction with the surface is dominated by the sulfur-copper bond in a like 1-atom bond configuration, explaining why the adsorption is isoenergetic.

For thiol molecules, the most stable configuration is in a parallel orientation to the surface (forming an angle of 90° with the normal of the surface). The molecules do not form covalent bonds with Cu atoms, the distance to the surface being 2.5-2.6 Å. The adsorption energies of MBT and MBI are similar and equal to -0.7 eV, mainly due to vdW interactions. When the thiol molecules are adsorbed according a 1-atom bond adsorption mode, the adsorption energy is considerably reduced and equal to about -0.1 eV

for both molecules, for two reasons: the Cu-SH bond is not so strong, and in this orientation, most atoms of the molecule have no significant vdW interaction with Cu.

To summarize the study of the molecule adsorption at low molecular density, the MBT and MBI molecules adsorb in the thiolate form according a 2-atom-Cu bonds mode (in a C_{2v} axis tilted orientation), forming two bonds with Cu atoms, involving the exocyclic S and a N atom, with an energy of adsorption of -1.21 eV (respectively -1.25 eV). For the 1-atom bond adsorption mode (through the exocyclic S), the adsorption energies are -0.82 and -0.87 eV.

The next steps of this work consist in studying if the layer density can impact molecules orientation which can form stable and dense layers with intermolecular interactions.

3.3. Adsorption of MBT and MBI monolayer on Cu(111) surface

The next step of this work was to model a Cu(111) surface covered by a monolayer of MBT and MBI. For that, we considered the 2 atoms and 1 atom adsorption modes as well as the thiolate and thione conformers of MBT and MBI. To build an adsorbed monolayer, we considered on the one hand the structure of atomic S adsorbed on Cu(111), the ($\sqrt{7} \times \sqrt{7}$) R19° structure [43] [44] [45] [46], with a S/Cu coverage of 2/7 as a starting point to anchor the molecules. This corresponds to a molecular density of 5 molecules/nm². On the other hand, we tried to find an epitaxy relationship between the dense layer formed by the molecules and the Cu surface. The lattice parameter of the hexagonal structure of Cu(111) is equal to 2.6 Å and that of the cell parameters of the perpendicular thione SAM formed by MBT and MBI are a= 4.7 and b = 5.8 Å, (with $\gamma= 60^\circ$), which means that a commensurate cell of the vertical SAM on the Cu(111) surface is a (9x9) superstructure for the copper and a (5x4) superstructure containing 20 molecules, for the molecules. Choosing a cell of this size would have induced too long computation times. So, we chose a compromise between computation time and realism of the model by defining a reduced cell size. For that, we adsorbed two molecules in a (3x3) cell, obtaining a density of 3.9 molecules/nm² for the organic monolayer, i.e. a density very near the density of the non-adsorbed SAM. To better study the influence of the increasing molecule density, we studied molecular adsorption also on (2x2), $\begin{pmatrix} 2 & 2 \\ 1 & -1 \end{pmatrix}$ and (4x4) cells. The details of the cells, of the molecular densities and calculations conditions are reported in the S.I.-1 section.

To compare all the results obtained for different cells, the results are expressed in eV/nm². As for the adsorption configuration at low density, results obtained for the thione and the thiolate forms are similar in geometry, but with a lower adsorption energy and therefore a more favored reaction for the thiolate form.

3.3.1. Results with MBT

The most stable monolayer is obtained for the thiolate form when the molecule is in the 2-atoms bonded adsorption mode, forming two S-Cu bonds, the sulfur atoms forming a (3x3) superstructure with a SAM density of 3.9 **molecule/nm²** (Figure 5). In this configuration, the adsorption energy is equal to -1.47 eV (-5.73 eV/nm²). We notice that at high coverage, not all surface sites are hollow sites, the molecule can accommodate with S atoms in a bridge position.

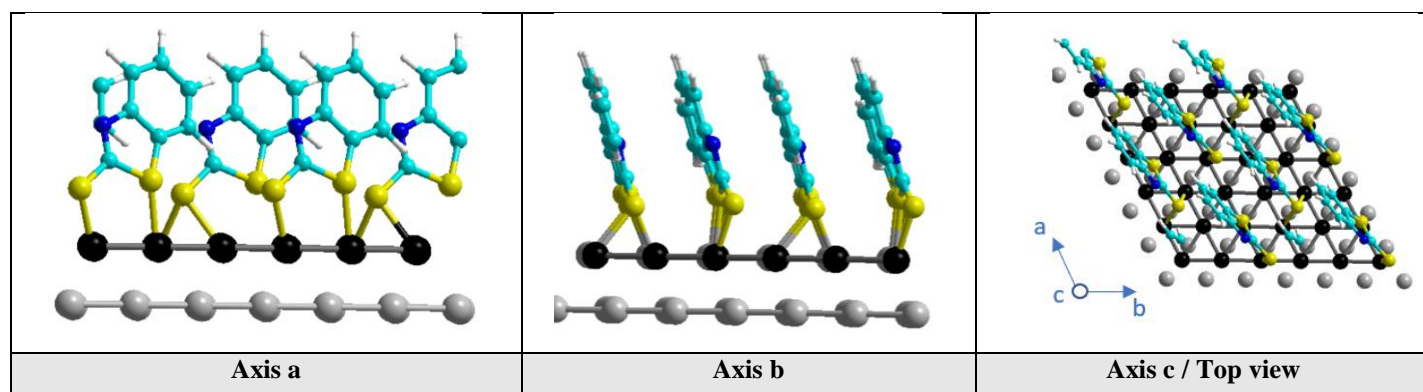


Figure 5: Most stable configuration obtained for the MBT thiolate SAM formation on Cu(111). A 2-atom bond configuration through the exo and endocyclic sulfurs is obtained in a (3x3) supercell. Views along axis a, b, and top view. Color code: light blue: C; dark blue: N; yellow: S; white: H, black and dark grey: Cu atoms

Figure 6 shows how the bonding mode to the surface evolves with the surface coverage. We observe that the adsorption energy increases in absolute value with coverage, until the molecular density is above 4 **molecule/nm²**, then the adsorption energy decreases (in absolute value). Also, we observe that the 2-atoms anchoring mode is more stable than the 1-atom one, until 4 **molecule/nm²**, and then the 1-atom bond mode is more stable. This is simply explained by the fact that at high molecular densities, the 1-atom anchoring mode allows to minimize the molecule-molecule steric hindrance. The molecular density of 4 **molecule/nm²** corresponds to the density of a full standalone MBT SAM (*vide infra*). Less stable configurations are reported in S.I.-7 section.

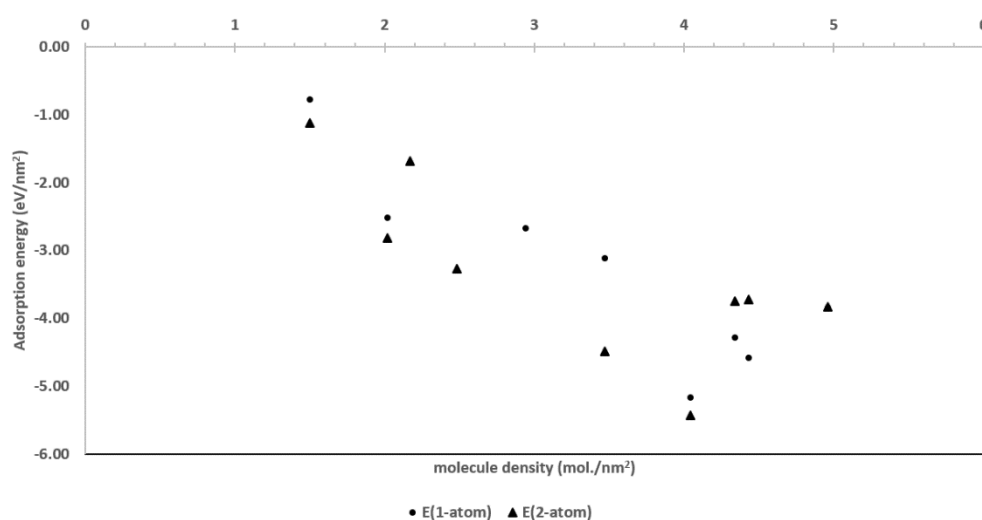


Figure 6: Adsorption energies of MBT thiolate on a Cu(111) surface as a function of molecular density, for the 1-atom bond and the 2-atom bond adsorption modes.

We obtained similar results with the thione configuration: the most stable monolayer is obtained when the molecules adsorb to the surface in the same configuration as the thiolate, making two Cu-S bonds, and organized with a (3 x 3) superstructure. In this case, the adsorption energy is equal to 1.40 eV (5.46 eV/nm²).

For the thiolate layer, open shell calculations were performed to verify that the system is not magnetic. We concluded that thiolates adsorbed in an anionic form. We indeed calculated a charge transfer from the metal to the molecule of 0.4 electrons, thus the thiolate acquires a negative charge. This charge is located mainly on the thiolate sulfur atom. The net charge acquired by the thiolate induces a considerable increase in the dipole moment as compared to the isolated or self-assembled neutral thiolate molecules.

3.3.2. Results with MBI

We found that the most stable thiolate monolayer (adsorption energy -1.70 eV or -6.56 eV/nm²), as for MBT, is formed when the molecule is in the 2-atom bond adsorption mode (S-Cu and N-Cu bonds are formed) in a (3x3) structure (Figure 7). The adsorbed thione structures are slightly less stable than the thiolate one, with -6.28 eV/nm².

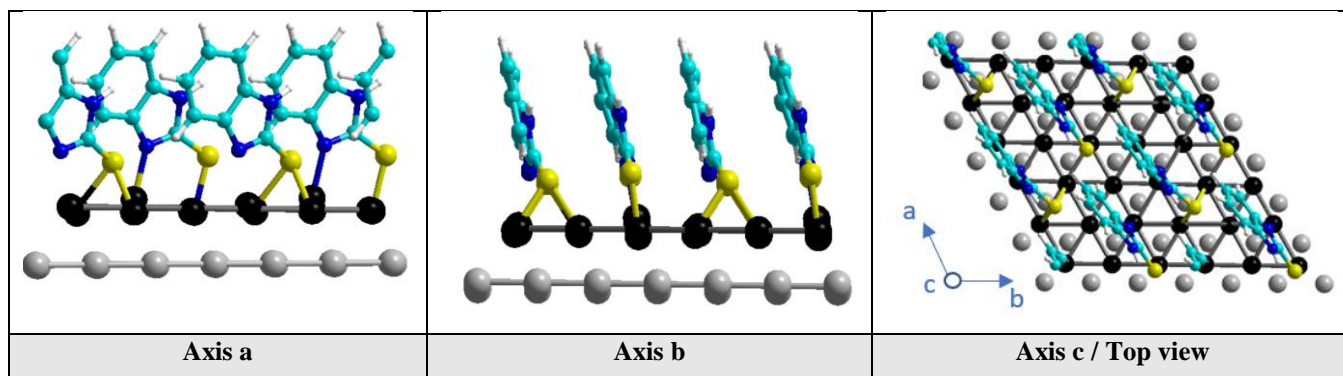
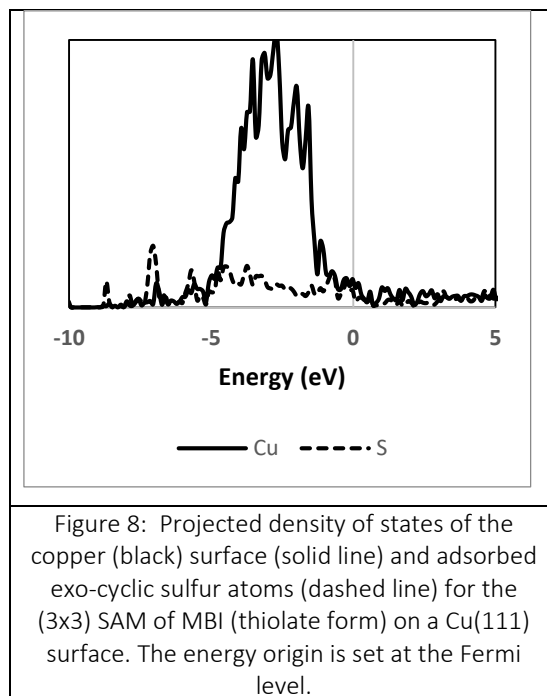


Figure 7: Most stable configuration obtained for the MBI thiolate SAM formation on Cu(111). A 2-atom bond configuration through the exocyclic sulfur and the deprotonated nitrogen is obtained in a (3x3) supercell. Views along axis a, b, and top view.

The electronic analysis of the MBI thiolate layer adsorbed on Cu is reported in Figure 8. The charge analysis shows that the thiolate molecules are negatively charged, -0.37 e, the main charge being localized on the Sulfur atom (-0.3 e). The S 2p and Cu 3d analysis indeed shows that electron density is shared between Cu and S (Figure 7). The integration of the DOS in the valence band gives 10 and 4.5 electrons for Cu and S, respectively. The two remaining electrons of S are located in the 1s band, at -15

eV (see S.I. section). We calculated that the dipole moment of the adsorbed molecule (5.78 D) in the adsorbed SAM is higher with respect to the isolated MBI molecule (4.3D) or standalone self-assembled MBI SAM (1.8 D). The Z-projected dipole moment is 1.9 D.



4. Conclusive Remarks

In the present paper, the study of adsorption of MBT and MBI in thiol, thiolate and thione forms on Cu(111) has been investigated. The results have shown that both molecules adsorb at low and high molecular density in a 2-atom bond adsorption mode. We found that the driving force for the monolayer formation is the epitaxy relationship between the honeycomb structures of the close packed SAM with the one of Cu(111). We found that the best structure formed is commensurate with a (3x3) Cu(111) superstructure.

As for the molecular form of the adsorbed MBT and MBI, the calculations suggest that the thiolate form, is favored at low and high molecule density. We calculate that the MBI layer formation is more exothermic than the MBT one. Our calculations predict thus that adsorption from the gas phase favors the thiolate adsorption of both molecules and that the formation of a full layer is slightly more favored for MBI. The higher adsorption energy **magnitude** suggests that MBI would act as a better corrosion inhibitor than MBT on metallic copper.

At the interface with water, in the pH range where the Cu metal is non-oxidized (low pHs), the predominant form of the molecules is the thione form. Our calculations suggest that adsorption occurs in the thiolate form and that full layers of MBT and MBI are formed. However, the reaction involves

the formation of one proton and one electron, thus is pH and electrochemical potential dependent. More work on the stability domains of thiolate adsorbed on Cu at the interface with water will be done in an incoming work.

5. Acknowledgments

The authors thank SOCOMORE for funding and GENCI for high performance calculations in the national (CINES) center under the A0040802217.

The raw/processed data required to reproduce these findings cannot be shared at this time due to technical or time limitations.

6. References

- [1] M. Kendig, S. Jeanjaquet, R. Addison, and J. Waldrop, "Role of hexavalent chromium in the inhibition of corrosion of aluminium alloys," *Surf. coatings Technol.*, vol. 140, pp. 58–66, 2001.
- [2] J. Sinko, "Challenges of chromate inhibitor pigments replacement in organic coatings," *Prog. Org. Coatings*, vol. 42, pp. 267–278, 2001.
- [3] R. M. Palou, O. Olivares-Xomelt, and N. V. Likhanova, "Environmentally friendly corrosion inhibitors," *Green Corros. Inhib. theory Pract.*, pp. 257–303, 2011, doi: 10.1002/9781118015438.ch7.
- [4] P. B. Raja and M. G. Sethuraman, "Natural products as corrosion inhibitor for metals in corrosive media - A review," *Mater. Lett.*, vol. 62, no. 1, pp. 113–116, 2008, doi: 10.1016/j.matlet.2007.04.079.
- [5] G. Gece, "The use of quantum chemical methods in corrosion inhibitor studies," *Corros. Sci.*, vol. 50, no. 11, pp. 2981–2992, 2008, doi: 10.1016/j.corsci.2008.08.043.
- [6] I. B. Obot, D. D. Macdonald, and Z. M. Gasem, "Density functional theory (DFT) as a powerful tool for designing new organic corrosion inhibitors: Part 1: An overview," *Corros. Sci.*, vol. 99, pp. 1–30, 2015, doi: 10.1016/j.corsci.2015.01.037.
- [7] D. Costa and P. Marcus, "Adsorption of Organic Inhibitor Molecules on Metal and Oxidized Surfaces Studied by Atomistic Theoretical Methods," in *Molecular Modeling of Corrosion Processes*, C. D. Taylor and P. Marcus, Eds. John Wiley & Sons, 2015, pp. 125–156.
- [8] M. Finšgar, A. Lesar, A. Kokalj, and I. Milošev, "A comparative electrochemical and quantum chemical calculation study of BTAH and BTAOH as copper corrosion inhibitors in near neutral chloride solution," *Electrochim. Acta*, vol. 53, no. 28, pp. 8287–8297, 2008, doi: 10.1016/j.electacta.2008.06.061.
- [9] A. Kokalj, S. Peljhan, and I. Milos, "What Determines the Inhibition Effectiveness of ATA , BTAH , and BTAOH Corrosion Inhibitors on Copper ?," *JACS*, vol. 132, pp. 16657–16668, 2010, doi: 10.1002/maco.201005645.
- [10] A. Kokalj, "Is the analysis of molecular electronic structure of corrosion inhibitors sufficient to predict the trend of their inhibition performance," *Electrochim. Acta*, vol. 56, no. 2, pp. 745–755, 2010, doi: 10.1016/j.electacta.2010.09.065.
- [11] J. C. Marconato and L. O. Bulho, "A spectroelectrochemical study of the inhibition of the electrode process on copper by 2- mercaptobenzothiazole in ethanolic solutions," *Electrochim. Acta*, vol. 43, no. 7, pp. 771–780, 1998.

- [12] T. Shahrabi, H. Tavakholi, and M. G. Hosseini, "Corrosion inhibition of copper in sulphuric acid by some nitrogen heterocyclic compounds," *Anti-Corrosion Methods Mater.*, vol. 54, no. 5, pp. 308–313, 2007, doi: 10.1108/00035590710822161.
- [13] L. P. Kazansky, I. A. Selyaninov, and Y. I. Kuznetsov, "Adsorption of 2-mercaptobenzothiazole on copper surface from phosphate solutions," *Appl. Surf. Sci.*, vol. 258, no. 18, pp. 6807–6813, 2012, doi: 10.1016/j.apsusc.2012.03.097.
- [14] M. Finšgar and D. Kek Merl, "An electrochemical, long-term immersion, and XPS study of 2-mercaptobenzothiazole as a copper corrosion inhibitor in chloride solution," *Corros. Sci.*, vol. 83, pp. 164–175, 2014, doi: 10.1016/j.corsci.2014.02.016.
- [15] M. Finšgar, "2-Mercaptobenzimidazole as a copper corrosion inhibitor: Part II. Surface analysis using X-ray photoelectron spectroscopy," *Corros. Sci.*, vol. 72, pp. 90–98, 2013, doi: 10.1016/j.corsci.2013.03.010.
- [16] G. Xue, X. Y. Huang, J. Dong, and J. Zhang, "The formation of an effective anti-corrosion film on copper surfaces from 2-mercaptobenzimidazole solution," *J. Electroanal. Chem. Interfacial Electrochem.*, vol. 310, no. 1–2, pp. 139–148, 1991.
- [17] R. Subramanian and V. Lakshminarayanan, "Effect of adsorption of some azoles on copper passivation in alkaline," *Corros. Sci.*, vol. 44, no. 3, pp. 535–554, 2002, doi: 10.1016/S0010-938X(01)00085-3.
- [18] D. Chadwick and T. Hashemi, "Electron spectroscopy of corrosion inhibitors: Surface films formed by 2-mercaptobenzothiazole and 2-mercaptobenzimidazole on copper," *Surf. Sci.*, vol. 89, no. 1–3, pp. 649–659, 1979, doi: 10.1016/0039-6028(79)90646-0.
- [19] J. Li, "Inhibition Film Formed by 2-mercaptobenzothiazole on Copper Surface and Its Degradation Mechanism in Sodium Chloride Solution," *Int. J. Electrochem. Sci.*, vol. 11, pp. 10690–10705, 2016, doi: 10.20964/2016.12.46.
- [20] S. Sun, Y. Geng, L. Tian, S. Chen, Y. Yan, and S. Hu, "Density functional theory study of imidazole, benzimidazole and 2-mercaptobenzimidazole adsorption onto clean Cu (1 1 1) surface," *Corros. Sci.*, vol. 63, pp. 140–147, 2012, doi: 10.1016/j.corsci.2012.05.024.
- [21] I. B. Obot, Z. M. Gasem, and S. A. Umoren, "Understanding the mechanism of 2-mercaptobenzimidazole adsorption on Fe (110), Cu (111) and Al (111) surfaces: DFT and molecular dynamics simulations approaches," *Int. J. Electrochem. Sci.*, vol. 9, no. 5, pp. 2367–2378, 2014.
- [22] N. Kovačević, I. Milošev, and A. Kokalj, "The roles of mercapto, benzene, and methyl groups in the corrosion inhibition of imidazoles on copper: II. Inhibitor–copper bonding," *Corros. Sci.*,

- vol. 98, pp. 457–470, 2015, doi: 10.1016/j.corsci.2015.05.006.
- [23] P. M. Niamien, F. K. Essy, A. Trokourey, A. Yapi, H. K. Aka, and D. Diabate, “Correlation between the molecular structure and the inhibiting effect of some benzimidazole derivatives,” *Mater. Chem. Phys.*, vol. 136, pp. 59–65, 2012, doi: 10.1016/j.matchemphys.2012.06.025.
- [24] M. K. Awad, M. R. Mustafa, and M. M. Abouelnga, “Quantum chemical studies and atomistic simulations of some inhibitors for the corrosion of al surface,” *Prot. Met. Phys. Chem. Surfaces*, vol. 52, no. 1, pp. 156–168, 2016, doi: 10.1134/S2070205116010032.
- [25] J. P. Perdew *et al.*, “Atoms , Molecules , Solids , and Surfaces : Applications of the Generalized Gradient Approximation for Exchange and Correlation,” *Phys. Rev.*, vol. 46, no. 11, pp. 6671–6687, 1992, doi: 10.1103/PhysRevB.46.6671.
- [26] J. P. Perdew, K. Burke, and M. Ernzerhof, “Generalized gradient approximation made simple,” *Phys. Rev.*, vol. 77, no. 18, pp. 3865–3868, 1996, doi: 10.1103/PhysRevLett.77.3865.
- [27] G. Kresse and J. Furthmiiller, “Efficiency of ab-initio total energy calculations for metals and semiconductors using a plane-wave basis set,” *Comput. Mater. Sci.*, vol. 6, pp. 15–50, 1996.
- [28] G. Kresse and J. Furthmüller, “Efficient iterative schemes for ab-initio total energy calculations using a plane-wave basis set,” *Phys. Rev.*, vol. 54, no. 16, pp. 11169–11186, 1996, doi: 10.1103/PhysRevB.54.11169.
- [29] G. Sun, J. Kürti, P. Rajczy, M. Kertesz, J. Hafner, and G. Kresse, “Performance of the Vienna ab initio simulation package (VASP) in chemical applications,” *J. Mol. Struct. THEOCHEM*, vol. 624, pp. 37–45, 2003.
- [30] G. Kresse and D. Joubert, “From ultrasoft pseudopotentials to the projector augmented-wave method,” *Phys. Rev. B*, vol. 59, no. 3, pp. 11–19, 1999.
- [31] S. Grimme, T. O. Chemie, and O. I. D. U. Münster, “Semiempirical GGA-Type Density Functional Constructed with a Long-Range Dispersion Correction,” *J. Comput. Chem.*, vol. 27, no. 15, pp. 1787–1799, 2006, doi: 10.1002/jcc.
- [32] S. Grimme, J. Antony, S. Ehrlich, and H. Krieg, “A consistent and accurat ab initio parametrization of density functional dispersion correction (DFT-D) for the 94 elements H-Pu,” *J. Chem. Phys.*, vol. 132, pp. 154104–154119, 2010, doi: 10.1063/1.3382344.
- [33] D. R. Line, *CRC Handbook of Chemistry and Physics*, 74th ed. Boca Raton, FL, 1993.
- [34] M. Poberžnik, F. Chiter, I. Milošev, P. Marcus, D. Costa, and A. Kokalj, “DFT study of n-alkyl carboxylic acids on oxidized aluminum surfaces: From standalone molecules to self-assembled-monolayers,” *Appl. Surf. Sci.*, vol. 525, no. 146156, 2020.

- [35] W. Tang, E. Sanville, and G. Henkelman, "A grid-based Bader analysis algorithm without lattice bias," *J. Phys. Condens. Matter*, vol. 21, no. 8, p. 084204, 2009.
- [36] N. Kovačević and A. Kokalj, "DFT Study of Interaction of Azoles with Cu(111) and Al(111) Surfaces: Role of Azole Nitrogen Atoms and Dipole–Dipole Interactions," *J. Phys. Chem. C*, vol. 115, no. 49, pp. 24189–24197, 2011.
- [37] S. Stoyanov, I. Petkov, L. Antonov, and T. Stoyanova, "Thione-thiol tautomerism and stability of 2- and 4-mercaptopyridines and 2-mercaptopyrimidines," *Can. J. Chem.*, vol. 68, pp. 1482–1489, 1989.
- [38] T. A. Mohamed, A. M. Mustafa, W. M. Zoghaib, M. S. Afifi, and R. S. Farag, "Reinvestigation of benzothiazoline-2-thione and 2-mercaptobenzothiazole tautomers : Conformational stability , barriers to internal rotation and DFT calculations," *J. Mol. Struct. THEOCHEM*, vol. 868, pp. 27–36, 2008, doi: 10.1016/j.theochem.2008.07.037.
- [39] A. L. R. Silva and M. D. M. C. Ribeiro, "Energetic , structural and tautomeric analysis of 2-mercaptobenzimidazole: an experimental and computational approach," *J. Therm. Anal. Calorim.*, vol. 129, no. 3, pp. 1679–1688, 2017, doi: 10.1007/s10973-017-6353-x.
- [40] N. Sandhyarani, G. Skanth, S. Berchmans, V. Yegnaraman, and T. Pradeep, "A Combined Surface-Enhanced Raman – X-Ray Photoelectron Spectroscopic Study of 2-mercaptobenzothiazole Monolayers on Polycrystalline Au and Ag Films," *J. Colloid Interface Sci.*, vol. 209, pp. 154–161, 1999.
- [41] A. A. A. Boraie and I. T. Ahmed, "Acid Dissociation Constants of Some Mercaptobenzazoles in Aqueous-Organic Solvent Mixtures," *J. Chem. Eng. Data*, vol. 9568, no. 96, pp. 787–790, 1996.
- [42] W. T. Geng, J. Nara, and T. Ohno, "Adsorption of benzene thiolate on the (111) surface of M (M = Pt , Ag , Cu) and the conductance of M / benzene dithiolate / M molecular junctions : a first-principles study," *Thin Solid Films*, vol. 465, pp. 379–383, 2004, doi: 10.1016/j.tsf.2004.06.083.
- [43] J. L. Domange and J. Oudar, "Structure et conditions de formation de la couche d'adsorption du soufre sur le cuivre," *Surf. Sci.*, vol. 11, pp. 124–142, 1968.
- [44] N. P. Prince, D. L. Seymour, M. J. Ashwin, C. F. Mcconville, D. P. Woodruff, and R. G. Jones, "A SEXAFS and X-RAY standing wave study of the Cu(111) ($\sqrt{7} \times \sqrt{7}$)R19° surface: adsorbate-substrate and adsorbate-adsorbate registry," *Surf. Sci.*, vol. 230, pp. 13–26, 1990.
- [45] L. Ruan, I. Stensgaard, F. Besenbacher, and E. Laegsgaard, "A scanning tunneling microscopy study of the interaction of S with the Cu (111) surface," *Ultramicroscopy*, vol. 42–44, pp. 498–504, 1992.

[46] M. Foss *et al.*, "Sulfur induced Cu₄ tetramers on Cu (111)," *Surf. Sci.*, vol. 388, pp. 5–14, 1997.